

# Gravitational Lensing Properties of Cosmological Black Holes

Alexander F. Zakharov<sup>1,2</sup>, Salvatore Capozziello<sup>3,4</sup>,  
Cosimo Stornaiolo<sup>3,4</sup>

<sup>1</sup>*Institute of Theoretical and Experimental Physics, Moscow, Russia*

<sup>2</sup>*Bogoliubov Laboratory of Theoretical Physics, JINR, Dubna, Russia*

<sup>3</sup>*Università di Napoli, Naples, Italy*

<sup>4</sup>*INFN, Sezione di Napoli, Naples, Italy*

SQS-15, 5 August 2015, BLTP, JINR, Dubna, Russia

# Chandrasekhar's Nobel prize talk

The mathematical theory of black holes is a subject of immense complexity; but its study has convinced me of the basic truth of the ancient mottoes, and

The simple is the seal of the true

Beauty is the splendour of truth.

**Hypermassive black holes are elsewhere!**

## An ultraluminous quasar with a twelve-billion-solar-mass black hole at redshift 6.30

Xue-Bing Wu<sup>1,2</sup>, Feige Wang<sup>1,2</sup>, Xiaohui Fan<sup>2,3</sup>, Weimin Yi<sup>4,5,6</sup>, Wenwen Zuo<sup>7</sup>, Fuyan Bian<sup>8</sup>, Linhua Jiang<sup>2</sup>, Ian D. McGreer<sup>3</sup>, Ran Wang<sup>9</sup>, Jinyi Yang<sup>1,2</sup>, Qian Yang<sup>1,2</sup>, David Thompson<sup>9</sup> & Yuri Beletsky<sup>10</sup>

So far, roughly 40 quasars with redshifts greater than  $z \approx 6$  have been discovered<sup>1–5</sup>. Each quasar contains a black hole with a mass of about one billion solar masses ( $10^9 M_{\odot}$ )<sup>6,7,8–13</sup>. The existence of such black holes when the Universe was less than one billion years old presents substantial challenges to theories of the formation and growth of black holes and the coevolution of black holes and galaxies<sup>14</sup>. Here we report the discovery of an ultraluminous quasar, SDSS J10013.021 280225.8, at redshift  $z = 6.30$ . It has an optical and near-infrared luminosity a few times greater than those of previously known  $z < 6$  quasars. On the basis of the deep absorption trough<sup>15</sup> on the blueside of the Lyman- $\alpha$  emission line in the spectrum, we estimate the proper size of the ionized proximity zone associated with the quasar to be about 26 million light years, larger than found with other  $z < 6.1$  quasars with lower luminosities<sup>16</sup>. We estimate (on the basis of a near-infrared spectrum) that the black hole has a mass of  $\sim 1.23 \times 10^{10} M_{\odot}$ , which is consistent with the  $1.33 \times 10^{10} M_{\odot}$  derived by assuming an Eddington-limited accretion rate.

High-redshift quasars have been efficiently selected using a combination of optical and near-infrared colours<sup>17</sup>. We have carried out a systematic survey of quasars at  $z < 6$ , using photometry from the Sloan Digital Sky Survey (SDSS)<sup>17</sup>, the two Micron All Sky Survey (2MASS)<sup>18</sup> and the Wide-field Infrared Survey Explorer (WISE)<sup>19</sup>, resulting in the discovery of a significant population of luminous high-redshift quasars. SDSS J10013.021 280225.8 (hereafter J1001 2802) was selected as a high-redshift quasar candidate owing to its red optical colour (with SDSS AB magnitudes  $i_{AB} = 20.846 \pm 0.06$  and  $z_{AB} = 18.336 \pm 0.03$ ) and photometric redshift of  $z < 6.3$ . It has bright detections in the 2MASS J, H and K<sub>s</sub> bands with Vega magnitudes of 17.006  $\pm$  0.20, 15.986  $\pm$  0.19 and 15.206  $\pm$  0.16, respectively; it is also strongly detected in WISE, with Vega magnitudes in W1 to W4 bands of 14.456  $\pm$  0.03, 13.636  $\pm$  0.03, 11.716  $\pm$  0.21 and 8.986  $\pm$  0.44, respectively (see Extended Data Figs 1 and 2 for images in different bands). Its colour in the two bluest WISE bands, W1 and W2, clearly differentiates it from the bulk of stars in our Galaxy<sup>20</sup>. The object was within the SDSS-III imaging area. It is close to the colour selection boundary of SDSS  $z < 6$  quasars<sup>17</sup>, but was assigned to low priority earlier because of its relatively red  $z_{AB} = 2$  colour and its bright apparent magnitudes. It is undetected in both radio and X-ray bands by the wide-area, shallow survey instruments.

Initial optical spectroscopy on J1001 2802 was carried out on 29 December 2013 with the Lijiang 2.4-m telescope in China. The low-resolution spectrum clearly shows a sharp break at about 8,800 Å, consistent with a quasar at a redshift beyond 6.2. Two subsequent optical spectroscopic observations were conducted on 9 and 24 January 2014 respectively with the 6.5-m Multiple Mirror Telescope (MMT) and the twin 8.4-m mirror Large Binocular Telescope (LBT) in the USA. The Lyman- $\alpha$  (Ly $\alpha$ ) lines shown in the spectra confirm that J1001 2802 is a quasar at a redshift of 6.30  $\pm$  0.01 (see Fig. 1 and Methods for details).

We use the multiwavelength photometry to estimate the optical luminosity at rest-frame wavelength 3,000 Å ( $L_{3000}$ ), which is consistent with that obtained from K-band spectroscopy (see below). The latter gives a more reliable value of  $(3.156 \pm 0.47) \times 10^{47}$  erg s<sup>-1</sup>, adopting a  $\Lambda$ CDM cosmology with Hubble constant  $H_0 = 70$  km s<sup>-1</sup> Mpc<sup>-1</sup>, matter density parameter  $\Omega_M = 0.30$  and dark energy density parameter  $\Omega_{\Lambda} = 0.7$ . Assuming an empirical conversion factor from the luminosity at 3,000 Å to the bolometric luminosity<sup>21</sup>, this gives  $L_{bol} = 5.153 \pm 1.623 \times 10^{48}$  erg s<sup>-1</sup>  $\approx 4.293 \times 10^{12} L_{\odot}$  (where  $L_{\odot}$  is the solar luminosity). We obtain a similar result when estimating the bolometric luminosity from the Galactic extinction corrected absolute magnitude at rest-frame 14,500 Å, which is  $M_{1450,AB} = 2.29266 \pm 0.20$ . The luminosity of this

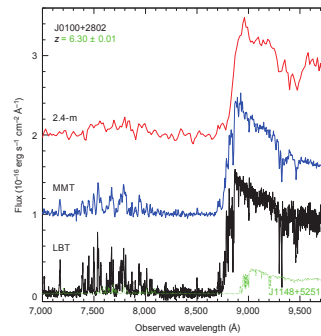


Figure 1 | The optical spectra of J1001 2802. From top to bottom, spectra taken with the Lijiang 2.4-m telescope, the MMT and the LBT (in red, blue and black colours), respectively. For clarity, two spectra are offset upward by one and two vertical units. Although the spectral resolution varies from very low to medium, in all spectra the Ly $\alpha$  emission line, with a rest-frame wavelength of 1,216 Å, is redshifted to around 8,900 Å, giving a redshift of 6.30. J1001 2802 is a weak-line quasar with continuum luminosity about four times higher than that of SDSS J11481 5251 (in green on the same flux scale)<sup>1</sup>, which was previously the most luminous high-redshift quasar known at  $z < 6.42$ .

<sup>1</sup>Department of Astronomy, School of Physics, Peking University, Beijing 100871, China. <sup>2</sup>Kavli Institute for Astronomy and Astrophysics, Peking University, Beijing 100871, China. <sup>3</sup>Steward Observatory, University of Arizona, Tucson, Arizona 85721-0065, USA. <sup>4</sup>Tunman Observatories, Chinese Academy of Sciences, Kunming 650011, China. <sup>5</sup>University of Chinese Academy of Sciences, Beijing 100049, China. <sup>6</sup>Key Laboratory for the Structure and Evolution of Celestial Objects, Chinese Academy of Sciences, Kunming 650011, China. <sup>7</sup>Shanghai Astronomical Observatory, Chinese Academy of Sciences, Shanghai 200030, China. <sup>8</sup>Mount Stromlo Observatory, Research School of Astronomy and Astrophysics, Australian National University, Weston Creek, Australian Capital Territory 2611, Australia. <sup>9</sup>Large Binocular Telescope Observatory, University of Arizona, Tucson, Arizona 85721, USA. <sup>10</sup>Las Campanas Observatory, Carnegie Institution of Washington, Colina el Pino, Casilla 601, La Serena, Chile.

Figure 1: Hypermassive black hole with mass  $M = 12 \times 10^9 M_{\odot}$  at redshift  $z = 6.3$  (Nature, February 2015). More than 40 SMBHs with masses  $M \sim 10^9 M_{\odot}$  at redshifts  $z > 6$ .

– Typeset by Foil<sub>TEX</sub> –

# Introduction

The Universe at scales less than 100 Mpc shows a spongy structure where together with regions with structure of galaxies there are void regions where there are underdense distribution of galaxies or where they are totally absent.

The existence of these cosmological voids, discovered first in the 80s of the last century, set the question of their actual extension and of their shape. And of their origin.

The analysis of their physical properties has been done using Void finders, i.e. by using codes which defined their shapes and their actual extensions. The most recent results assign an average radius of 25 Mpc and an approximately spherical shape. There is a galaxy underdensity in the

borders of the voids, but the central part is apparently without any visible matter, i.e. optically void.

As follows from an analysis reported by (Peebles 2001), the small dispersion of galaxy peculiar velocities indicates that there must be more matter in voids than expected. Then the problem is to establish the nature of this dark matter.

A simple model to explain contemporarily the presence of this dark matter and void formation is to admit that there have been large perturbations, eventually produced by a long inflationary period, that collapsed into black holes (CBH) and that voids have been created by the cosmological expansion around these CBHs. To describe the resulting model, in previous papers, the Einstein-Straus Swiss cheese model has been used. In this case dark matter can totally be identified with the CBHs, i.e. "ordinary" black holes with huge dimensions. In order to compensate the void region these black holes must have a mass of the order of  $10^{14}M_{\odot}$  (the mass value is consistent

with density fluctuations (Tegmark & Zaldarriaga 2002, Tegmark 2004).

In a perfect Swiss Cheese model, a CBH will not have any direct interaction with the other structures except for contributing to the energy density of the universe and participating to the collective cosmological expansion. To explain some deviations from this scenario which are in the actual observations, one has to consider the presence of peculiar velocities for galaxies and some perturbation of this scenario. Otherwise the CBHs can be detected only through their lensing properties.

Lensing properties of CBHs have been discussed previously by simulating them numerically, but in this paper we go deeper in the theoretical analysis looking for the signature of the presence of a CBH.

An existence of a number supermassive black holes with redshifts  $z > 6$  with black hole masses  $10^9 M_{\odot}$  is a real challenge for existing theoretical models (Volonteri 2012, Wu et al. 2015) and there is an opinion that it

looks like an anomaly and one has to introduce a non-standard accretion physics or assume a formation of massive seeds (Melia 2014). Therefore, in principle, such seeds could exist not only in centers of quasars and galaxies where an accreting baryonic matter is shining and indicating their locations, but also in voids, which could have a complex internal structure (Zeldovich et al. 1982, Kopylov et al. 2002, Aragon-Calva & Szalay 2013), so voids could be a key player in this game similarly to vacuum in quantum field theory and cosmology.



# Schwarzschild lens model

## Basic Relations

The Schwarzschild lens model was studied by Einstein (1936). Here we will remind basic notations and relations which we will use in our studies. The gravitational lens equation can be written in the following form (see also (Schneider, Ehlers, Falco, 1992) for reference)

$$\vec{\eta} = D_s \vec{\xi} / D_l - D_{ls} \vec{\Theta}(\vec{\xi}), \quad (1)$$

where  $\eta, \xi$  are vectors determining positions of sources and images in the source and image planes, respectively,  $D_s, D_l, D_{ls}$  are angular diameter distances between source and observer, lens and observer, lens and source respectively. For the Schwarzschild lens we have (Schneider, Ehlers, Falco,

1992)

$$\vec{\Theta}(\vec{\xi}) = 4GM\vec{\xi}/c^2|\vec{\xi}|^2. \quad (2)$$

If a source is located at the origin ( $\vec{\eta} = 0$ ) we have a definition for the Einstein – Chwolson radius (Chwolson 1924; Schneider, Ehlers, Falco, 1992)

$$\xi_0 = \sqrt{4GMD_l D_{ls}/(c^2 D_s)}. \quad (3)$$

If  $D_s \gg D_l$  ( $D_s \approx D_{ls}$ ) then

$$\xi_0 = \sqrt{4GMD_l/c^2} \quad (4)$$

We will introduce also the Einstein – Chwolson angle  $\theta_0 = \xi_0/D_l$ .

If we can re-write the gravitational lens equation in the dimensionless form with dimensionless variables

$$\vec{x} = \vec{\xi}/\xi_0, \quad \vec{y} = D_s \vec{\eta}/(\xi_0 D_l), \quad \vec{\alpha} = \vec{\Theta} D_{ls} D_l / (D_s \xi_0) \quad (5)$$

then we have

$$\vec{y} = \vec{x} - \vec{\alpha}(\vec{x}) \quad (6)$$

or

$$\vec{y} = \vec{x} - \vec{x}/x^2. \quad (7)$$

The gravitational lens equation has two solutions

$$x^{\pm} = y \left[ 1/2 \pm \sqrt{1/4 + 1/y^2} \right] \quad (8)$$

or

$$x^+ = y \left[ \frac{1}{2} + \sqrt{\frac{1}{4} + \frac{1}{y^2}} \right], \quad (9)$$

$$x^- = y \left[ \frac{1}{2} - \sqrt{\frac{1}{4} + \frac{1}{y^2}} \right], \quad (10)$$

$$l = x^+ + |x^-| = 2y \sqrt{\frac{1}{4} + \frac{1}{y^2}}, \quad (11)$$

where  $l$  is a dimensionless distance between these two solutions. Clearly that one image is located outside of the Einstein – Chwolson ring  $x^+$ , another one is located inside the Einstein – Chwolson ring  $x^-$ . We select orientation of axis to have  $\vec{y} = (|y|, 0)$ . For small  $y \approx 0$  we can write solutions in the

form

$$x^{\pm} = \pm 1 + \frac{1}{2}y + O(y^2), \quad (12)$$

therefore, for sources with a small impact parameter  $y$ , an image size in radial direction is squeezing in 2 times (see Figs. 2, 3). More precisely, squeezing in radial direction is determined by the derivative

$$\frac{dx^{\pm}}{dy} = \frac{1}{2} \pm \frac{y}{\sqrt{4+y^2}} = \frac{1}{2} \pm \frac{y}{2} + O(y^2). \quad (13)$$

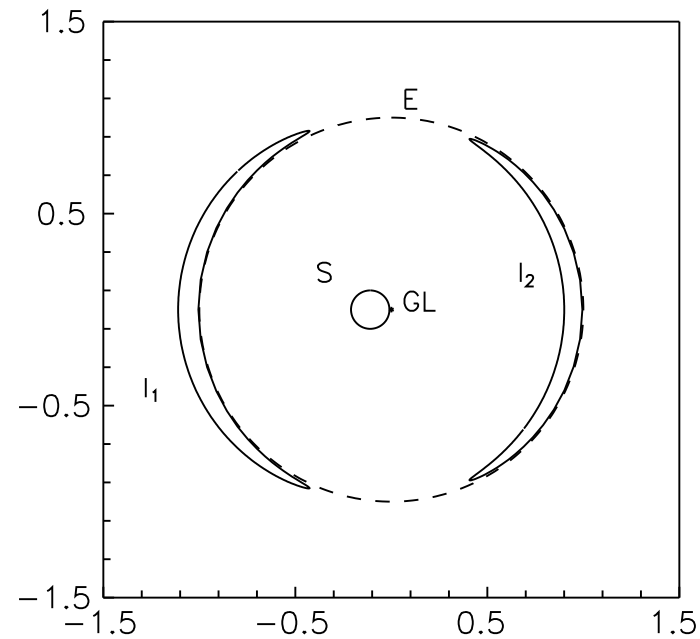


Figure 2: Image of a circular source for the Schwarzschild lens. Radius of source  $r = 0.1$ , impact parameter  $y = 0.11$ . It is clear that radius of source is roughly in 2 times larger than widths of images in radial direction.

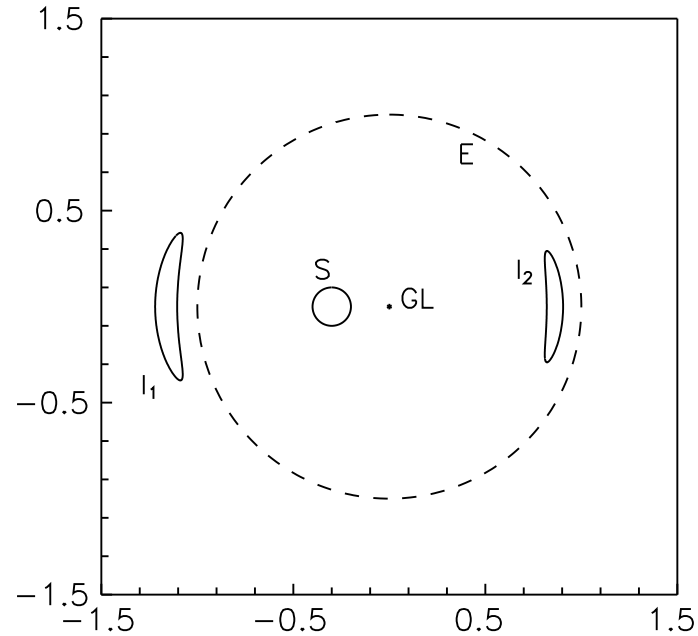


Figure 3: Image of a circular source for the Schwarzschild lens. Radius of source  $r = 0.1$ , impact parameter  $y = 0.3$ . It is also clear that radius of source is larger than widths of images in radial direction.

We will remind also relations for amplification of the Schwarzschild lens. Let us introduce angles describing positions of images and a source in the Einstein – Chwolson angle units, namely,  $\vec{\theta} = \vec{\xi}/D_l$ ,  $\vec{\beta} = \vec{\eta}/D_s$ . In these



case amplification of gravitational lens is the Jacobian describing a ratio between an solid angles of image area and a source area, or more formally

$$\mu = \frac{\Delta\omega}{\Delta\omega_0} = \left| \det \frac{d\vec{\beta}}{d\vec{\theta}} \right|^{-1} = \left| \det \frac{d\vec{y}}{d\vec{x}} \right|^{-1}. \quad (14)$$

So, we have

$$\vec{y} = \vec{\beta}/\theta_0, \quad \vec{x} = \vec{\theta}/\theta_0. \quad (15)$$

For the case of the mapping

$$x_{\pm}^{\vec{}} \mapsto \vec{y} \quad (\vec{y} = (y_1, 0)), \quad (16)$$

we evaluate Jacobians

$$\mu_{\pm} = \left| \det \frac{d\vec{x}^{\pm}}{d\vec{y}} \right|. \quad (17)$$

Since only diagonal terms of the Jacobian are non-vanishing, we calculate

$$\left. \frac{\partial x_1^{\pm}}{\partial y_1} \right|_{(y_1,0)} = \frac{1}{2} \left( 1 \pm \frac{y_1}{\sqrt{4 + y_1^2}} \right), \quad (18)$$

$$\left. \frac{\partial x_2^{\pm}}{\partial y_2} \right|_{(y_1,0)} = \frac{1}{2} \left( 1 \pm \frac{\sqrt{4 + y_1^2}}{y_1} \right), \quad (19)$$

or

$$\mu_{\pm} = \frac{1}{4} \left( \frac{y_1}{\sqrt{4 + y_1^2}} + \frac{\sqrt{4 + y_1^2}}{y_1} \pm 2 \right), \quad (20)$$

for ratio of amplifications we have

$$\frac{\mu_+}{\mu_-} = \left( \frac{\sqrt{4 + y_1^2} + y_1}{\sqrt{4 + y_1^2} - y_1} \right)^2, \quad (21)$$

We can calculate an asymptotic behavior if  $y_1 \rightarrow 0$  (Schneider, Ehlers, Falco, 1992)

$$\mu_+ = \frac{1}{2y_1} + \frac{1}{2} + O(y_1), \quad (22)$$

$$\mu_- = \frac{1}{2y_1} - \frac{1}{2} + O(y_1), \quad (23)$$

$$\frac{\mu_+}{\mu_-} = 1 + y_1 + O(y_1^2). \quad (24)$$

If  $y_1 \rightarrow \infty$ , then

$$\mu_+ = 1 + y_1^{-4} + O(y_1^{-6}), \quad (25)$$

$$\mu_- = y_1^{-4} + O(y_1^{-6}), \quad (26)$$

$$\frac{\mu_+}{\mu_-} = y_1^4 + O(y_1^0). \quad (27)$$

## Blinded region and relative brightness of images

Gravitational lensing leads to shifts of image positions (in respect to positions of sources) and changes visible brightness of images. As it was noted earlier, if an angular distance between a position of source and position of lens increases the secondary image is fainter and its position approaches a position of lens. Since primary images are always located outside of the Einstein–Chwolson ring, a blinded region is formed inside the ring, where only secondary images could be but they are too faint to be detectable.

One can introduce different definitions for radius of blinded region (compare with a definition of the region done by (Stornaiolo et al. 2007)). We will evaluate a critical position of a source for the case if a secondary image has the same brightness as a source, namely, we will calculate  $y_{cr}$

from the condition (it means that for  $y > y_{cr}$  a secondary image is fainter than a source and its position is closer to the center)

$$\mu_- = \frac{1}{4} \left( \frac{y_{cr}}{\sqrt{y_{cr}^2 + 4}} + \frac{\sqrt{y_{cr}^2 + 4}}{y_{cr}} - 2 \right) = 1. \quad (28)$$

It is easy to find that in this case

$$y_{cr} = \sqrt{\frac{(2 - \sqrt{2})(\sqrt{2} - 1)}{2}} \approx 0.35. \quad (29)$$

Substituting  $y_{cr}$  into Eq. (10), we obtain

$$|x_{cr}^-| = y_{cr} \left| \frac{1}{2} - \sqrt{\frac{1}{4} + \frac{1}{y_{cr}^2}} \right| = \sqrt{\frac{(2 - \sqrt{2})(\sqrt{2} - 1)}{2}} (1 + \sqrt{2}) \approx 0.84. \quad (30)$$

We can define  $y_{cr}$  in another way, for example, from the relation

$$\mu_- = \frac{1}{2}\mu_+, \quad (31)$$

but in this case we arrive at the same relation (29) for  $y_{cr}$ .

Practically, a physical meaning of the blinded region is the following. If we could observe a distant galaxy behind a void in absence of the black hole and if the angular position of the galaxy from a center of the black hole is  $y < y_{cr}$ , then even a secondary image is not fainter than the source and we could observe a pair of images with a distance between them according to Eq. (11).

## Ellipticity of images

It is well-known that for weak gravitational lensing evaluation of shear from ellipticity of background images is used to reconstruct surface mass density distribution (Mellier 1999, Amendola et al. 1999). However, if a gravitational lens model is known we can evaluate ellipticity as a function of a position of an image. Below we will give simple formulas for a brighter image assuming impact parameter  $y$  and size of circular source  $r$  are small in comparison with the Einstein – Chwolson radius  $\xi_0$ . In the framework of these approximation we have

$$\frac{r}{y} = \frac{R_1}{x^+}, \quad (32)$$



where  $R_1$  is the semi-major axis of the bright image. Since  $x^+ \approx 1 + y/2$ ,

$$R_1 = \frac{r}{y}(1 + y/2), \quad (33)$$

and we have for semi-minor axis of the bright image

$$R_2 \approx r/2, \quad (34)$$

therefore, an ellipticity of the image as a function of a source position  $y$  and a position of the image  $x^+$

$$\epsilon = \frac{R_2}{R_1} = \frac{y}{2(1 + y/2)} = 1 - 1/x^+. \quad (35)$$

If an average ellipticity evaluated in a standard way for suspected region for cosmological black hole may be fitted with Eq. (35), it could be a signature

of Schwarzschild black hole, because other gravitational lens models have different dependence of ellipticity on a a position of the image  $x^+$ .

## Bulk distribution of lens mass

In this section we will consider the singular isothermal sphere model as a reference approach for a comparison with the Schwarzschild lens model (Schneider, Ehlers, Falco, 1992). As a probable alternative for a cosmological black hole a bulk concentration of dark matter could act as a gravitational lens.

We will use a mass density distribution in the form

$$\rho(r) = \rho_0 \frac{a_0^2}{r^2}, \quad (36)$$

where  $r$  is a current distance from the center,  $\rho_0$  is a density at a distance  $a_0$  from the center,  $a_0$  is a radius of the lens (practically, we assume that the

relation for mass density distribution is valid for impact parameters  $\xi < a_0$ . The Eq. (36) is applicable to describe flat rotation curves in galaxies.

We can evaluate a surface mass density from Eq. (36).

$$\begin{aligned} \Sigma_{DM}(\vec{\xi}) &= 2\rho_0 \int_0^{\sqrt{a_0^2 - \xi^2}} \frac{a_0^2}{\xi^2 + h^2} dh = \\ & 2\rho_0 \frac{a_0^2}{\xi} \arctan \frac{\sqrt{a_0^2 - \xi^2}}{\xi}. \end{aligned} \quad (37)$$

In the case if  $a_0 \gg \xi$ ,  $\Sigma(\vec{\xi}) \longrightarrow \pi\rho_0 \frac{a_0^2}{\xi}$ .

In this case we can re-write the gravitational lens equation in the

following form

$$\vec{\eta} = \frac{D_s}{D_l} \vec{\xi} - D_{ls} \vec{\hat{\theta}}_{DM}(\vec{\xi}), \quad (38)$$

where

$$\vec{\hat{\theta}}_{DM}(\vec{\xi}) = \int_{R^2} d^2\xi' \frac{4G\Sigma_{DM}(\vec{\xi}')}{c^2} \frac{\vec{\xi} - \vec{\xi}'}{|\vec{\xi} - \vec{\xi}'|^2}. \quad (39)$$

It is known (Schneider, Ehlers, Falco, 1992) that the gravitational lens model (36) has two drawbacks: there is a singularity at  $r = 0$  (an infinite density is clearly not too appropriate point of the model). However, one can see that a mass does not become infinite. 2) The second drawback is infinite mass of the lens if we consider infinite values of  $a_0$ . However, for a consideration of the gravitational lens effect mass in a region outside a

selected impact parameter  $\xi' > \xi$  To write the equation lens equation in dimensionless form, we use a characteristic distance  $a_0$ , which corresponds to the lens mass,

$$M = 4\pi\rho_0 a_0^3, \quad (40)$$

If we introduce dimensionless variables

$$\vec{x} = \frac{\vec{\xi}}{a_0}, \vec{y} = \frac{\vec{\eta}}{\eta_0},$$

where  $\eta_0 = a_0 \frac{D_s}{D_d}$ ,  $\Sigma_{cr} = \frac{c^2 D_s}{4\pi G D_d D_{ds}}$

$$\vec{\hat{\alpha}}(\vec{x}) = \frac{1}{\pi} \int_{R^2} d^2 x' k(\vec{x}') \frac{\vec{x} - \vec{x}'}{|\vec{x} - \vec{x}'|^2}.$$

and

$$k(\vec{x}) = \frac{\Sigma(a_0\vec{x})}{\Sigma_{cr}}.$$

Then the surface mass density can be written in the form

$$\Sigma(\vec{\xi}) = \pi\rho_0\frac{a_0^2}{\xi} \quad (41)$$

Since surface mass density is axisymmetric, the equation of gravitational lens can be written in the scalar form (Schneider, Ehlers, Falco, 1992)

$$y = x - \alpha(x) = x - \frac{m(x)}{x}, \quad (42)$$

where

$$m(x) = 2 \int_0^x x' dx' k(x').$$

We remind that the  $k(x)$  has the form

$$k(x) = \frac{k_0}{x}, \quad (43)$$

where

$$k_0 = \frac{\pi \rho_0 a_0}{\Sigma_{cr}} = \frac{M}{a_0^2} \frac{4\pi G D}{c^2}, \quad (44)$$

and

$$D = \frac{D_l D_{ls}}{D_s}. \quad (45)$$



So, the lens equation is the form

$$y = x - R_0 \frac{x}{|x|}, \quad (46)$$

where  $R_0 = 2k_0$ . If we normalized all distances in the lens and the source plane to  $R_0$ , namely if we introduce variables  $\hat{y} = y/R_0$ ,  $\hat{x} = x/R_0$ , then lens equation has a rather simple form

$$\hat{y} = \hat{x} - \frac{\hat{x}}{|\hat{x}|}, \quad (47)$$

In subsequent analysis the symbol  $\wedge$  is omitted. It is easy to see that Eq. (47) coincides with the lens equation for a singular isothermal sphere model (Schneider, Ehlers, Falco, 1992).

We will remind basic properties lens equation (47). First we remind solutions for the gravitational lens equation. Without a losses of generality

we assume that  $y > 0$ . If  $y < 1$ , then the Eq. (47) has two solutions  $x_+ = y + 1, x_- = y - 1$ . If  $y > 1$ , there is only one solution  $x = y + 1$ . As usual amplification of gravitational lens is reversely proportional Jacobian for the gravitational lens mapping (47), namely,

$$A(\vec{x}) = \frac{\partial \vec{y}}{\partial \vec{x}}, \quad (48)$$

or

$$A_{ij} = \frac{\partial y_i}{\partial x_j}, \quad (49)$$

Then an amplification factor is determined from the relation

$$\mu(\vec{x}) = \frac{1}{\det A(\vec{x})}. \quad (50)$$

Since we have spherically symmetric distribution then we have the following relation for the Jacobian

$$\det A(\vec{x}) = 1 - \frac{1}{|x|}, \quad (51)$$

therefore, an amplification is equal

$$\mu = \frac{|x|}{|x| - 1}. \quad (52)$$

Clearly, the critical curve is determined by the relation  $|x| = 1$  (i.e. unit circumference). Remind if critical curves are circumferences they called like tangential (Schneider, Ehlers, Falco, 1992). A caustic curve degenerates into one point  $y = 1$ .

It is easy to understand distortions of images with the gravitational lens. Clearly that images are not stretching (or squeezing) in radial direction,

but there is stretching in tangential direction according to (52). Remind that for the Schwarzschild lens for  $y \ll 1$ , we have squeezing of images approximately in 2 times in radial direction and similar stretching ( $\approx 1/y$ ) in a tangential direction. One can understand it from formal geometrical analysis. If we consider the case  $y > 1$ , then

$$\mu(y) = \mu(x_+) = \frac{y+1}{y} = 1 + \frac{1}{y}. \quad (53)$$

If we consider the case  $0 < y < 1$ , then

$$\mu(x_+) = \frac{|x_+|}{|x_+| - 1} = \frac{y+1}{y} = 1 + \frac{1}{y}, \quad (54)$$

$$\mu(x_-) = \frac{|x_-|}{|x_-| - 1} = \frac{y-1}{y}. \quad (55)$$

In this case since  $\mu(x_-) < 0$ , then amplification for second image is  $|\mu(x_-)| = \frac{1}{y} - 1$ , and the total amplification for two images is

$$\mu(y) = \mu(x_+) + |\mu(x_-)| = \frac{2}{y}. \quad (56)$$

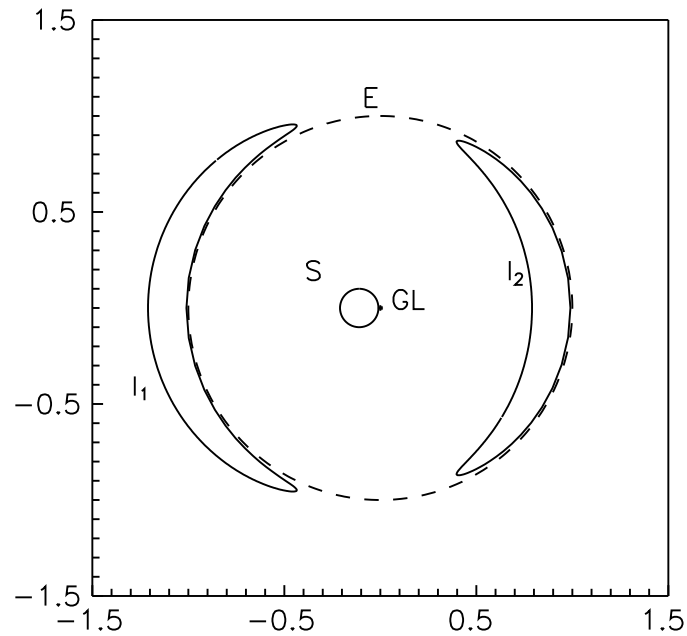


Figure 4: Image of a circular source for the transparent lens. Radius of source  $r = 0.1$ , impact parameter  $y = 0.11$ . It is clear that radius of source is the same as widths of images in radial direction.

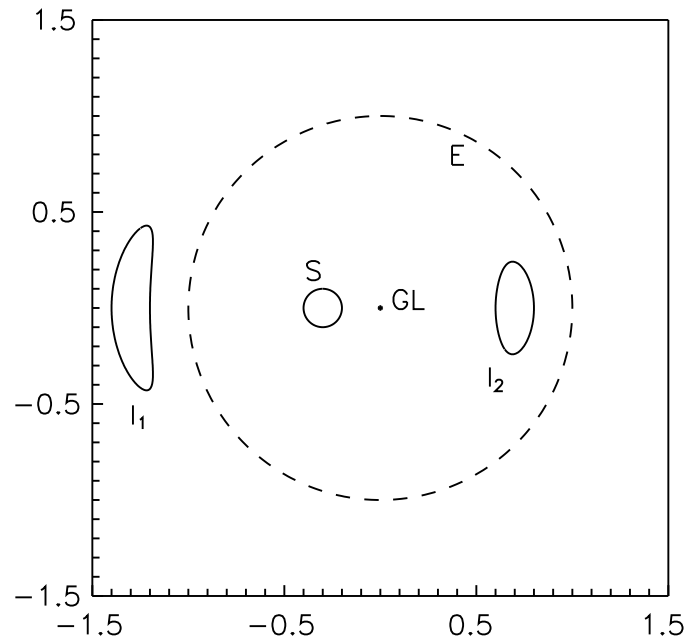


Figure 5: Image of a circular source for the transparent lens. Radius of source  $r = 0.1$ , impact parameter  $y = 0.3$ . It is also clear that radius of source is the same as widths of images in radial direction.

## Ellipticity of images

We can evaluate ellipticity as a function of a position of an image. Below we will give simple formulas for a brighter image assuming impact parameter  $y$  and size of circular source  $r$  are small in comparison with the  $a_0$ . Therefore, we have

$$\frac{r}{y} = \frac{R_1}{x^+}, \quad (57)$$

where  $R_1$  is the semi-major axis of the bright image. Since  $x^+ = 1 + y_{DM}$ ,

$$R_1 = \frac{r}{y}(1 + y_{DM}), \quad (58)$$



and we have for the semi-minor axis of the bright image

$$R_2 = r/2, \quad (59)$$

therefore, an ellipticity of the image as a function of a source position  $y$  and a position of the image  $x^+$

$$\epsilon = \frac{R_2}{R_1} = \frac{y_{DM}}{(1 + y_{DM})} = 1 - 1/x^+. \quad (60)$$

Therefore, in spite of different dependence of ellipticity on a position of source, we have the same dependence on  $x^+$  with a position of source  $y_{DM} = y/2$  (it means that a source is in 2 times closer to the center of lens, in this case it mimics an ellipticity for the Schwarzschild lens).

But clearly, if we use weak gravitational lensing technique (Mellier 1999, Amendola et al. 1999), then contours with a constant mass density may

help to reconstruct a mass density distribution which are definitely different for the Schwarzschild lens and a transparent lens with a bulk distribution of mass (Leclercq et al. 2015).

## Non-singular model for non-compact lens

We approximate the density of mass distribution of a DM (neutralino) in the following form

$$\rho_{Ne}(r) = 2\rho_0 \frac{r_c^2}{r^2 + r_c^2}, \quad (61)$$

where  $r$  is the current value of a distant from the stellar center,  $\rho_0$  is a mass density for a boundary of a core (or for a distance  $r_c$  from a center),  $r_c$  is the radius of the core. So we use the non-singular isothermal sphere model (or the model of an isothermal sphere with a core) The dependence is the approximation of the dependence which has been considered (Gurevich et al, 1995, 1996, 1997; Zakharov & Sazhin 1996, 1997), where the authors considered the model of noncompact object with a core. It is clear that the

singular (degenerate) dependence (36) is the limiting dependence of (61) for  $r_c \rightarrow 0$ . Gravitational lensing for the mass density distribution (61) have been considered by (Hinshaw & Krauss 1987), where they used a different approach.

So, it is not difficult to obtain surface density mass, according to expression (61)

$$\Sigma(\vec{\xi}) = 4\rho_0 r_c^2 \int_0^{\sqrt{R_x^2 - \xi^2}} \frac{a_0^2}{\xi^2 + h^2 + r_c^2} dh = 4\rho_0 \frac{r_c^2}{\sqrt{\xi^2 + r_c^2}} \operatorname{atan} \frac{\sqrt{R_x^2 - \xi^2}}{\sqrt{\xi^2 + r_c^2}}. \quad (62)$$

In the case, if  $R_0 \gg \xi$ , then  $\Sigma(\vec{\xi}) \longrightarrow 2\pi\rho_0 \frac{r_c^2}{\sqrt{\xi^2 + r_c^2}}$ . In that case the lens equation has the following form

$$\vec{\eta} = \frac{D_s}{D_d} \vec{\xi} - D_{ds} \vec{\alpha}_{NeS}(\vec{\xi}), \quad (63)$$

where  $D_s$  is the distance from the source to the observer,  $D_d$  is the distance from the gravitational lens to the observer,  $D_{ds}$  is the distance from the source to the gravitational lens, vectors  $(\vec{\eta}, \vec{\xi})$  define a deflection on the plane of the source and the lens respectively and

$$\vec{\alpha}_{NeS}(\vec{\xi}) = \int_{R^2} d^2\xi' \frac{4G\Sigma(\vec{\xi}')}{c^2} \frac{\vec{\xi} - \vec{\xi}'}{|\vec{\xi} - \vec{\xi}'|^2}. \quad (64)$$

We calculate the lens mass

$$M_x = 8\pi\rho_0 r_c^2 \int_0^{R_x} \frac{r^2 dr}{r^2 + r_c^2} = 8\pi\rho_0 r_c^2 \left( R_x - r_c \operatorname{atan} \frac{R_x}{r_c} \right) \approx 8\pi\rho_0 r_c^2 R_x. \quad (65)$$

We use the characteristic value of a radius  $r_c$ , corresponding the lens "mass"  $M_x = 8\pi\rho_0 r_c^2 R_x$ , thus we obtain the lens equation in the dimensionless form. We introduce the dimensionless variables by the following way  $\vec{x} = \frac{\vec{\xi}}{r_c}$ ,  $\vec{y} = \frac{\vec{\eta}}{\eta_0}$ ,  $\eta_0 = r_c \frac{D_s}{D_d}$ ,

$$\Sigma_{cr} = \frac{c^2 D_s}{4\pi G D_d D_{ds}}, \quad k(\vec{x}) = \frac{\Sigma(a_0 \vec{x})}{\Sigma_{cr}}, \quad \vec{\alpha}(\vec{x}) = \frac{1}{\pi} \int_{R^2} d^2 x' k(\vec{x}') \frac{\vec{x} - \vec{x}'}{|\vec{x} - \vec{x}'|^2}.$$

As we supposed that surface density is an axial symmetric function then the equation of the gravitational lens may be written in the scalar form (Schneider, Ehlers, Falco, 1992)

$$y = x - \alpha(x) = x - \frac{m(x)}{x}, \quad m(x) = 2 \int_0^x x' dx' k(x').$$

We recall that we have the following expression for the function  $k(x)$

$$k(x) = \frac{k_0}{\sqrt{1+x^2}},$$

$$k_0 = \frac{2\pi\rho_0 r_0}{\Sigma_{cr}} = \frac{2\pi M_x G D_d D_{ds}}{r_c R_x c^2 D_s} = \frac{\pi}{4r_c R_x} \frac{4GM_x D_d D_{ds}}{c^2 D_s} = \frac{\pi}{4} \frac{R_E^2}{r_c R_x}. \quad (66)$$

Hence, the lens equation has the following form (Zakharov, 1998, 1999)

$$y = x - D \frac{\sqrt{x^2 + 1} - 1}{x}, \quad (67)$$

where  $D = 2k_0$ .

## A qualitative analysis of the gravitational lens equation

We will show that the gravitational lens equation has only one solution if  $D < 2$  and have three solutions if  $D > 2$  and  $y > y_{cr}$  (we consider the gravitational lens equation for  $y > 0$ ), where  $y_{cr}$  is a local maximal value of right hand of Eq. (67). It is possible to show that we determine the value  $x_{cr}$  which corresponds to  $y_{cr}$  using the following expression

$$x_{cr}^2 = \frac{2D - 1 - \sqrt{4D + 1}}{2}, \quad (68)$$

It is easy to see that according to (68)  $x_{cr}^2 > 0$  if and only if  $D > 2$  (the



same idea has been used qualitatively in Fig. 6 by Young et al. (1980)

$$y_{cr} = x_{cr} - D \frac{\sqrt{1 + x_{cr}^2} - 1}{x_{cr}}, \quad (69)$$

If we choose  $x_{cr} < 0$  then  $y_{cr} > 0$ . We suppose that  $y > 0$ . So, if  $D \leq 2$  then gravitational lens equation has only one solution; if  $D > 2$  then gravitational lens equation has single solution (if  $y > y_{cr}$ ), three distinct solutions (if  $y < y_{cr}$ ), one single solution and one double solution (if  $y = y_{cr}$ ). The right hand side of gravitational lens equation is shown in Fig. 6.

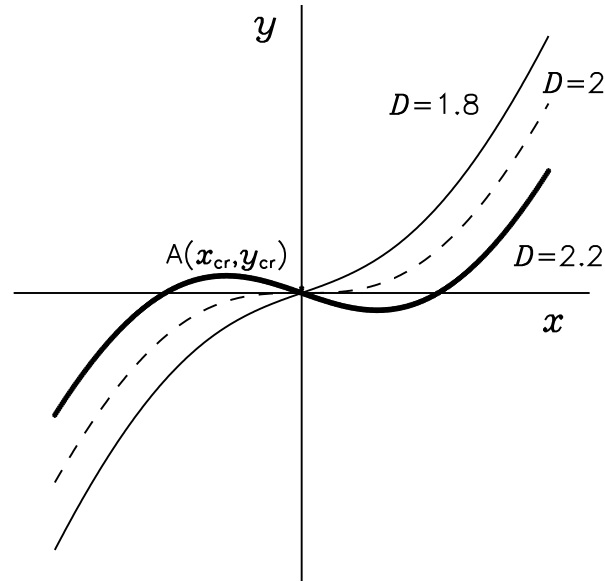


Figure 6: The right hand side of the gravitational lens equation for different values of the parameters  $D = 1.8, 2, 2.2$ .

It is possible to show that the gravitational lens equation is equivalent to the following equation

$$x^3 - 2yx^2 - (D^2 - y^2 - 2D)x - 2yD = 0, \quad (70)$$

jointly with the inequality

$$x^2 - yx + D > 0. \quad (71)$$

Thus it is possible to obtain the analytical solutions of the gravitational lens equation by the well-known way. We perform  $z = x - \frac{2y}{3}$  and obtain the incomplete equation of third degree

$$z^3 + pz + q = 0, \quad (72)$$

where  $p = 2D - D^2 - \frac{y^2}{3}$  and  $q = \frac{2y}{3} \left( \frac{y^2}{9} - D(D+1) \right)$ , so we have the following expression for the discriminant

$$Q = \left( \frac{p}{3} \right)^3 + \left( \frac{q}{2} \right)^2 = \frac{D^2}{27} [-y^4 + y^2(2D^2 + 10D - 1) + D(2 - D)^3]. \quad (73)$$

If  $Q \geq 0$  then Eq. (72) has the unique real solution (therefore the gravitational lens equation (67) has the unique real solution). We use Cardan expression for the solution

$$x = \sqrt[3]{-q/2 + \sqrt{Q}} + \sqrt[3]{-q/2 - \sqrt{Q}} + 2y/3. \quad (74)$$

We suppose the case  $D > 2$ . If  $y > y_{cr}$  then the gravitational lens equation has a single solution. If  $Q \geq 0$  then we use the expression (74) for the solution. If  $Q < 0$  then we have the following expression

$$x_k = 2\sqrt{-\frac{p}{3}} \cos \frac{\alpha + 2k\pi}{3} + \frac{2y}{3}, \quad (k = 0, 1, 2) \quad (75)$$

where

$$\cos \alpha = -\frac{q}{2\sqrt{-(p/3)^3}}, \quad (76)$$

and we select only one solution which corresponds to the inequality (71) which corresponds to  $k = 0$  in (75) because if the gravitational lens equation has only one solution then we have a positive solution  $x$  for a positive value of impact parameter  $y$  therefore there is the inequality  $x > y$  which is easy to see from (69). It is possible to check that maximal solution of (70) corresponds to  $k = 0$  therefore the solution is the solution of (69).

If  $y < y_{cr}$  then the gravitational lens equation has three distinct solutions and we use the Eqs. (75 – 76) to obtain the solutions.

We consider now the case  $D < 2$ . We know that the gravitational lens equation has the single solution for the case. If  $Q \geq 0$  then we use

the expression (74) for the solution. If  $Q < 0$  then we have the following expressions (75 – 76) and we select only one solution which corresponds to the inequality (71) which also corresponds to  $k = 0$  as in the previous case.

It is known that the magnification for the gravitational lens solution  $x_k$  is defined by the following expression

$$\mu_k = \left( 1 - \frac{D(\sqrt{1 + x_k^2} - 1)}{x_k} \right) \left( 1 + D \frac{\sqrt{1 + x_k^2} - 1}{x_k^2} - D \frac{1}{\sqrt{1 + x_k^2}} \right), \quad (77)$$

so the absolute value total magnification is equal

$$\mu_{\text{tot}}(y) = \sum |\mu_k|, \quad (78)$$

where the summation is taken over all solutions of gravitational lens equation for a fixed value  $y$ .

Similarly to the gravitational lens equation near cusp singularity we have three solutions of the gravitational lens equation, however, asymptotic behavior of algebraic sum of magnifications is different. Near the cusp type singularity we have asymptotically the so-called sum rule for magnifications (Schneider & Weiss 1992, Zakharov 1995, Mao & Schneider 1998)

$$\mu_1 + \mu_2 + \mu_3 = 0, \quad (79)$$

meanwhile near the fold singularity, we have clearly

$$\mu_0 + \mu_1 + \mu_2 = \mu_0, \quad (80)$$

since for fusing solutions  $(x_1, x_2)$  of the gravitational lens equation corresponding magnifications have the the same absolute value and the opposite parities near the fold singularity (Schneider, Ehlers, Falco, 1992).

## Possible observational features

If a cosmological black hole exists in a void, there are two stages in studying it as a strong gravitational lens. The first stage is to find gravitational lens systems in the void region. The second one is to confirm that it is a point-like gravitational lens (i.e. a Schwarzschild lens), and not an extended distribution of dark matter.

Since a region, where a secondary image is not demagnified, is rather large (Eq.29) for hypermassive black holes there is a high probability to find pairs of images formed by the black hole. If only one pair of images will be found it will be hard to prove that we a Schwarzschild lens (a hypermassive black hole), because, practically two parameters are observing: a ratio of brightness  $\mu^+/\mu^-$  and distance between images  $l$  and if a lens model is known as for our case (a Schwarzschild lens) we can evaluate its mass



and position of a source and position of images. But if several pairs with different distances between images will be found and for all of these systems it is obtained the same mass it will be a serious support that we have a Schwarzschild lens in this case because for bulk distribution of mass it would be very hard to expect that we will fit these data with a bulk density and with a small number of parameters. Besides, if there is a transparent lens in the void we expect that in general transparent gravitational lenses have to be asymmetric and the formation of an odd number of images (Schneider, Ehlers, Falco, 1992).

## Typical parameters for CBH lensing

Following Stornaiolo et al. (2007) we adopt CBH mass  $M = 10^{14} M_{\odot}$  and the distance to the void  $D_{void} = 50 Mpc$  (or we assume  $\Omega_{CBH} = 0.1$  and  $R_{void} \sim 20 Mpc$ , then Einstein – Chwolson ring is around is a few angular minutes, while shadow diameter (Falcke et al. 2000, Melia & Falcke 2001, Zakharov et al. 2005, 2012; Falcke & Markoff 2013, Zakharov 2014) is around a few  $10^{-2}$  angular seconds and we do not discuss an opportunity to find the small dark shadow inside a huge void.

**Thank you very much for  
your kind attention**